Laser-based excitation of nonlinear solitary waves in a chain of particles

Xianglei Ni,[1] Piervincenzo Rizzo,[1,*] and Chiara Daraio[2]

[1]*Department of Civil and Environmental Engineering, University of Pittsburgh, Pittsburgh, Pennsylvania 15261, USA*

[2]*Engineering and Applied Science, California Institute of Technology, 1200 East California Boulevard,*
MC 105-50, Pasadena, California 91125, USA

Highly nonlinear solitary waves (HNSWs) are stress waves that can form and travel in highly nonlinear systems. They are characterized by a constant spatial wavelength and by a tunable propagation speed, dependent on the wave amplitude. Conventionally, HNSW's are generated in one-dimensional chains of spherical particles by means of a mechanical impact. In this paper, we demonstrate that short-duration laser pulses can be used to generate HNSW's, and we characterize their propagating properties in terms of shape, speed, and duration. We compare the waves' characteristics with theoretical predictions, finding excellent agreement. In addition a simplified formulation is given to estimate the dynamic contact force generated by laser pulses onto the chain.

I. INTRODUCTION

Over the past decade, the study of highly nonlinear solitary waves (HNSWs) in closely packed chains of elastically interacting spherical particles (i.e., granular crystals) has drawn increased attention [1–18]. This interest has arisen from the ability to tune the level of nonlinearity (therefore the waves' duration, amplitude, and speed) by adding static precompression on the system or varying the particles' material and geometry [2,3,9]. This tunability makes the use of HNSWs suitable in engineering applications such as nondestructive testing (NDT) [11,19] or acoustic imaging [20].

Single HNSWs are commonly induced in one-dimensional granular crystals by mechanically impacting the first bead of the chain with a striker having the same mass of the particles composing the chain. In this study, we experimentally investigated the use of short-duration (∼ 8 ns) laser pulses to induce HNSWs in a one-dimensional chain of stainless-steel spheres. We analyzed the properties of the traveling waves using sensors placed in selected particles of the chain. The results were compared with the theoretical predictions based on the analysis of highly nonlinear waves provided by Nesterenko [2].

The use of pulsed-laser excitations to trigger the formation of HNSWs has practical advantages, such as noncontact coupling between the laser and the chain of particles. These advantages could be useful in applications where a remote placement of equipment or a complex geometrical arrangement of the chains is required (e.g., in NDT of materials), or for triggering multiple solitary waves in parallel chains (e.g., to generate sound bullets [20]).

II. BACKGROUND

In a one-dimensional chain of spherical particles, the interaction between two adjacent beads is governed by Hertz's law [2,3]. The combination of this nonlinear contact interaction and a zero tensile strength in the chain of spheres leads to the

formation and propagation of compact solitary waves [2]. In the long-wavelength limit, the speed of the solitary waves V_S depends on the maximum dynamic strain ξ_m [2] which, in turn, is related to the maximum force F_m between the particles in the discrete chain [10].

When the chain of beads is under a static precompression force F_0, the initial strain of the system is referred to as ξ_0. In the continuum approximation (long-wavelength limit), the speed of the solitary wave V_s has a nonlinear dependence on the normalized maximum strain $\xi_r = \xi_m/\xi_0$, or on the normalized force $f_r = F_m/F_0$ in the discrete case. Such a relationship is expressed by the following equation [2,9]:

$$
\begin{aligned}
V_S &= c_0 \frac{1}{(\xi_r - 1)} \left\{ \frac{4}{15}\left[3 + 2\xi_r^{5/2} - 5\xi_r\right] \right\}^{1/2} \\
&= 0.9314 \left(\frac{4E^2 F_0}{a^2 \rho^3 (1 - \nu^2)^2} \right)^{1/6} \frac{1}{\left(f_r^{2/3} - 1\right)} \\
&\quad \times \left\{ \frac{4}{15}\left[3 + 2f_r^{5/3} - 5f_r^{2/3}\right] \right\}^{1/2},
\end{aligned}
\tag{1}
$$

where c_0 is the wave speed in the chain initially compressed with a force F_0 in the limit $f_r = 1$, a is the diameter of the beads, and ρ, ν, and E are the density, Poisson's ratio, and Young's modulus of the material, respectively. When f_r is very large, Eq. (1) becomes

$$
V_S = 0.6802 \left(\frac{2E}{a\rho^{3/2}(1 - \nu^2)} \right)^{1/3} F_m^{1/6},
\tag{2}
$$

which represents the speed of a solitary wave in a "sonic vacuum" [2].

The shape of a solitary wave with a speed V_s in a "sonic vacuum" can be closely approximated by [2]

$$
\xi = \left(\frac{5V_s^2}{4c^2} \right) \cos^4 \left(\frac{\sqrt{10}}{5a} x \right),
\tag{3}
$$

where

$$
c = \sqrt{ \frac{2E}{\pi \rho (1 - \nu^2)} }
\tag{4}
$$

---
*Corresponding author: 942 Benedum Hall, 3700 O'Hara St., Pittsburgh, PA 15261, USA; pir3@pitt.edu

and x is the coordinate along the wave propagation direction.

III. EXPERIMENTAL SETUP

In our experiments, one-dimensional granular crystals were assembled by aligning 20 stainless-steel balls (Mc-Master Carr–Multipurpose Stainless Steel, Type 302) inside a vertical Teflon tube having an inner diameter equal to 4.8 mm. The diameter of each sphere was equal to 4.76 mm and the mass was 0.45 g. Two piezogauges made from lead zirconate titanate (square plates 0.27 mm thick and 2 mm wide) with nickel-plated electrodes and custom micro-miniature wiring were embedded inside two of the steel particles. The assembling and calibration of the instrumented particles were similar to that described in [2,6,9]. The sensor beads were positioned along the chain at the 9th and 14th position from the top, and connected to an oscilloscope. Signals were sampled at 10 MHz. To compare the experimental results with the theoretical predictions, the forces measured by the instrumented beads ($F_{m,e}$) were related to the dynamic contact forces (F_m) as described in [6].

A 10 Hz repetition rate Nd:YAG pulse laser operating at 1064 nm wavelength was used to excite stress waves in the chain of particles. The laser beam output diameter was equal to 7 mm. Through conventional optics [a 45° high-energy Nd:YAG mirror and a plano-convex (PCX) UV fused silica lens, 25.4 mm diameter, and 100 mm focal length], a $\sim$1-mm-diam beam, as measured using a laser alignment paper, was directed on the surface of the first particle of the chain. The laser was operated in single-shot mode. To apply variable amounts of static precompression on the chain of particles, we placed a polycarbonate sheet above the chain, loaded with variable balanced masses. To allow direct interaction of the laser beam with the first particle in the chain, a 3-mm-diameter hole was drilled in the center of the sheet. A schematic diagram of the experimental setup is presented in Fig. 1.

IV. LASER EXCITATION

The transfer of energy from a nanosecond optical pulse to a mechanical wave can occur by thermoelastic transduction or by ablation, depending on the intensity of the laser pulses and the surface properties of the illuminated targets. A thermoelastic stress is created when the laser energy density is low, such that
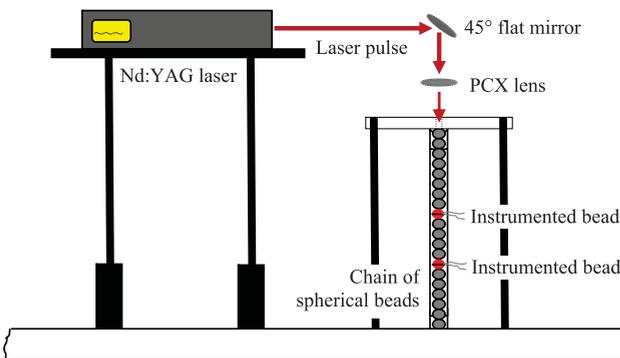
FIG. 1. (Color online) Schematic diagram of the experimental setup.

there is no material ablation or plasma formation on the surface of the object. In this regime, shear mechanical stresses are generated by the thermal expansion due to the sharp increase of the surface's temperature. Laser ablation is generated when the laser's power density is high, or when the surface of the illuminated medium is covered with a film of water or gel. In this case, the rapid vaporization (ablation) of the film at the surface, or the melting of a small portion of the medium's surface, induces high reaction pressures that can be considered similar to normal stress loading [21–23]. Picosecond light pulses have also been used to generate very short stress waves in films of different materials via thermal expansion [24].

In our experiments, we relied on the ablation of a controlled amount of water deposited with a syringe on the surface of the first bead to generate mechanical stresses in the chain of particles. To estimate the amount of mechanical stress transferred from the laser to the chain, we assume that the energy transfer occurs only through the ablation of the water droplet deposited on the first particle of the chain, and we describe the energy transfer using the equations that govern the ablation of water on a flat metallic surface [25]. The incident power density I of the pulsed laser is given by

$$I = \frac{E_L}{A\Delta t},$$ (5)

where E_L is the energy of the laser, Δt is the pulse duration, and A is the area of the pulse. The ablation of material from the surface produces a net stress in reaction against the sample [25] in the direction of the chain's axis. This stress can be calculated from the rate of change of momentum, i.e.,

$$\sigma = \frac{I_a^2}{\rho_w[L + C(T_v - T_0)]^2}.$$ (6)

In Eq. (6), I_a is the absorbed power density, ρ_w is the density of water, L is the water's latent heat of vaporization, C is the thermal capacity of water, T_v is the vaporization temperature of water, and T_0 is the ambient temperature (293 K) at which the experiment was conducted. For a polished mild steel irradiated by a 1064 nm laser pulse, the reflectivity coefficient R is equal to 0.63 [25] and the absorbed power density is equal to

$$I_a = I(1 - R).$$ (7)

The effective force F generated by ablating the water droplet on the metallic surface is equal to

$$F = \sigma A.$$ (8)

This force is analogous to the dynamic contact force generated by a striker impacting the top particle of the chain. If we assume that the amplitude of the pulse energy is constant over its 8 ns duration, then the mechanical impulse J transferred to the chain of particle is given by

$$J = F\Delta t.$$ (9)

The impulse J is equivalent to the impulse generated by a striker bead having the same mass of the particle chains and falling from an effective height h_{eq}. If we assume the values shown in Table I, the impulse of the laser is equivalent to a falling mass of 0.45 g from an effective height $h_{eq} = 21$ mm.

TABLE I. Parameters used to compute the net stress force generated by the ablation of a drop of water on the flat surface of polished mild steel.

Parameter	Value	Unit
E_L	150×10^{-3}	J
Pulse diameter	0.5×10^{-3}	m
Δt	8×10^{-9}	s
ρ_w	1000	Kg/m^3
L	2260×10^3	J/kg
C	4200	J/kg K
T_v	373	K

This estimate is in agreement with experimental measurements performed on the same chain of particles excited by a mechanical striker released from different heights [26]. In the study reported in [26], it was found that the average maximum dynamic contact force measured between the 7th and 12th sensor beads when the striker was released from ∼20 mm was equal to 21.44 N. As shown in the next section, in the present study the average maximum dynamic contact force measured between the 9th and 14th sensor beads was equal to 10.54 N when the laser pulse energy was 150 mJ. It is important to mention that the estimate of the effective drop height does not take into account the presence of losses and attenuation in the system, and it assumes that the laser pulse intensity is constant in time (a better approximation would be obtained considering a Gaussian-like pulse). In addition, the diameter of the laser pulse plays an important role: for example, a 1-mm-pulse diameter yields $h_{eq} = 1.4$ mm.

V. RESULTS

We investigated the effects of the beam intensity and of the precompression on the characteristics of the solitary waves. To determine the effects of the energy, we varied the laser's energy output between 120 and 190 mJ with 10 mJ increments. As the diameter of the beam impinging the top particle of the chain was equal to 1 mm, the energy can be straightforwardly related to the laser intensity expressed in J/cm^2. To study the effect of precompression, we used four different values of precompressive force: 0.049, 2.305, 3.384, and 5.150 N. These static preloads were applied placing balanced masses on the polycarbonate sheet. The values include the self-weight of the top 11 beads.

Typical time waveforms recorded by the two instrumented particles in the chain at four different values of precompression and 160 mJ laser energy (equivalent to an energy density of 20.37 J/cm^2) are shown in Fig. 2. For comparison, a cos^4 function Eq. (3) [2] was superimposed to the measured waveforms. As expected, at low values of precompressive force [Fig. 2(a)] the shape of the experimental pulse is in excellent agreement with predictions from the highly nonlinear theory. However, with an increasing amount of precompression with respect to the amplitude of the dynamic force $F_{m,e}$, the response of the chain shifts from the highly nonlinear regime toward the weakly nonlinear and linear response. This is evident from the appearance of an increasingly large tensile part of the pulse in Figs. 2(b)–2(d) and from the presence of additional oscillations following the leading pulse.

The speed of the HNSW was calculated by detecting the arrival time of the pulse's peak in the instrumented beads and knowing their relative distance in the chain. We compared
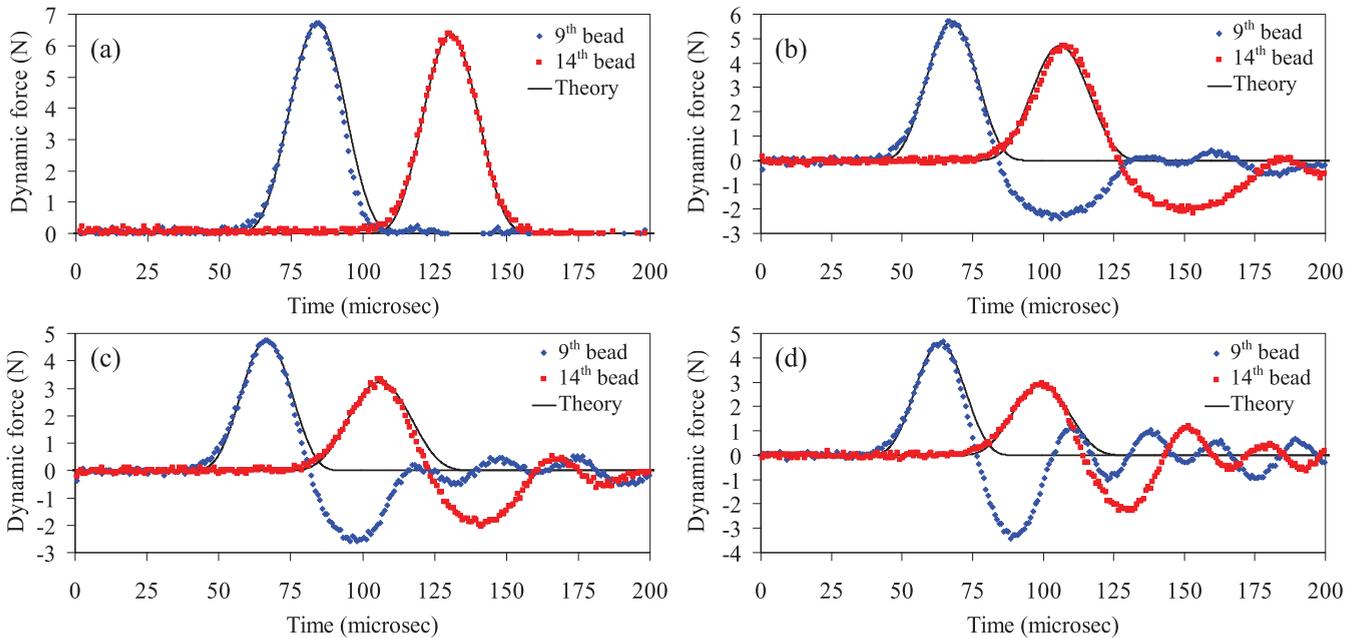
FIG. 2. (Color online) Comparison of the pulse shape obtained in experiments (dotted lines) with a theoretical cos^4 function (solid line). The first pulses (blue diamonds) represent the signal recorded by the sensor positioned in the ninth particle from left to right from the top of the chain. The second pulses (red squares) represent the signal recorded by the sensor positioned in the 14th particle from the top of the chain. The different panels indicate waveforms obtained at the same level of laser energy (160 mJ) but at different values of static precompression: (a) 0.049 N, (b) 2.305 N, (c) 3.384 N, and (d) 5.150 N.
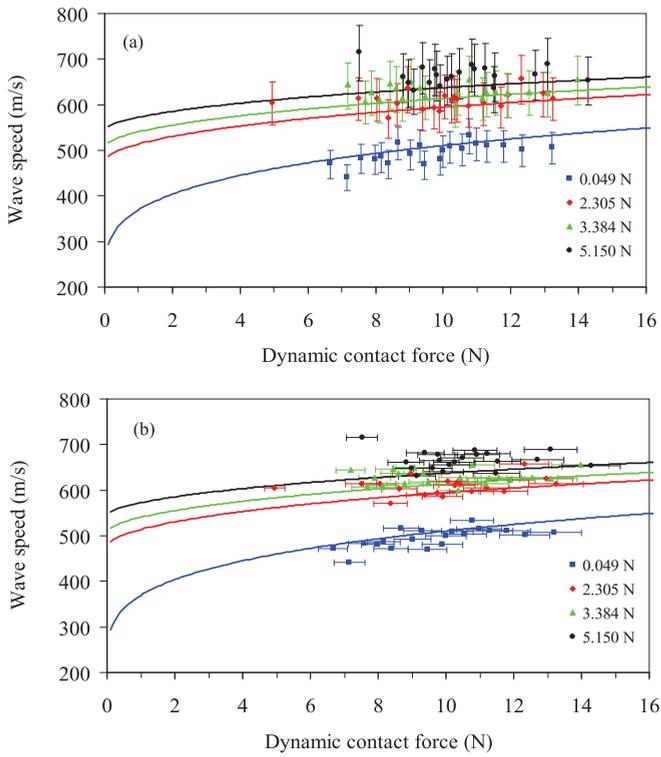
FIG. 3. (Color online) Wave speed as a function of the dynamic contact force at different amounts of static precompression. The experimental values are shown by solid dots (blue squares: 0.049 N; green triangles: 2.305 N; red diamonds: 3.384 N; and black circles: 5.150 N). The theoretical curves based on Eq. (1) for the different values of static precompression applied to the chain are represented by solid lines. From bottom line to upper line: 0.049, 2.305, 3.384, and 5.150 N. For clarity, we show two separate plots with vertical and horizontal error bars for the experimental points. In (a), the vertical error bars are the results of possible inaccuracy on the estimation of the peak's arrival time and on the measurement of the travel distance between the two piezosensors. In (b), the horizontal error bars are the results of accuracy of the sensors' calibration coefficients.

FIG. 4. (Color online) (a) Experimental plot showing the variation of the dynamic contact force as a function of the laser energy magnitude for four different levels of static precompression (blue squares: 0.049 N; green triangles: 2.305 N; red diamonds: 3.384 N; and black circles: 5.150 N). (b) Evolution of the traveling wave in the chain of stainless-steel beads excited by the laser pulse. The curves represent the force magnitude recorded by the instrumented beads positioned in the second, third, fourth, fifth, and eighth particle from left to right from the excitation site.

this speed with the amplitude of the traveling pulses. Figure 3 shows the HNSW's speed as a function of the dynamic contact force. To ensure repeatability of the results, each measurement at a given laser pulse energy was repeated ten times, for a total of 320 data points collected. For the sake of clarity, only a random subset of data out of 320 measurements is presented. The experimental wave velocities associated with the four levels of precompression were compared to the corresponding theoretical curves obtained from Eq. (1). The agreement between the experimental data and the theoretical prediction confirms that short-duration laser pulses can generate HNSWs.

The effect of the laser density on the characteristics of the propagating waves is shown in Fig. 4. Variations in the dynamic force amplitude as a function of the laser energy used to excite the pulses are shown in Fig. 4(a) for a value of static preload equal to 0.049 N. It is evident that the solitary-wave amplitude increases nonmonotonically with increased laser energy. For example, a decrease of the contact force is evident between 19.10 and 20.37 J/cm² for all four precompression forces tested. This suggests that the characteristics of the beam are

nonlinearly proportional to the laser energy output. Ongoing studies are investigating this phenomenon as possibly related to the interplay between ablative and thermoelastic effects in the illuminated particles. The vertical error bars reported in Fig. 4(a) represent the standard deviation associated with the ten measurements taken at each energy level. The scatter of the data is likely associated with the variable impulse generated during the water ablation. Although great care was taken in depositing the same amount of water at each measurement, variation in the liquid coating thickness on the particle might have occurred.

We also examined variations of the solitary-wave length as a function of the applied precompression and the amplitude of the traveling pulses. Experimental data, in agreement with theoretical prediction from the highly nonlinear wave theory [2], showed that the solitary-wave length does not change significantly (with a constant spatial duration of the leading pulses always measured at approximately five particles diameter).

Finally, we studied the initial formation and propagation of the solitary waves in the vicinity of the laser excitation. For these experiments, the position of the instrumented beads in the chain was changed systematically to allow the visualization of the pulse shape evolution in the vicinity of the excitation

site. Figure 4(b) shows the signals recorded by the sensor bead placed in the second through fifth and eighth position from the top. The shape of the signals varied dramatically in the immediate vicinity of the excitation source, and the formation of the solitary wave becomes evident after approximately four particles from the excitation point. The high-frequency components visible at the second and third bead are related to the ultrasonic bulk waves confined inside the particles, traveling at ~5.8 km/s.

VI. CONCLUSIONS

This work demonstrates that short-duration pulsed laser beams can be used for the remote generation of highly nonlinear solitary waves and oscillatory signals in chains of spherical particles with variable precompression. The evolution of the excited pulse shape within the chain was studied experimentally, showing a rapid formation of a stationary wave after the fourth particle from the excitation site. The experimentally measured dependence of the solitary-wave velocity on the pulse amplitude was found to be in excellent agreement with the theoretical predictions for all precompression levels tested. The paper also presents a simplified model that predicts the amount of dynamical contact force that can be generated in a chain of particles using a pulsed laser. This model can be used to estimate the mechanical pulse transferred to the granular system. This laser-based noncontact method for nonlinear wave generation could be employed in different engineering applications.

[1] V. F. Nesterenko, J. Appl. Mech. Tech. Phys. **24**, 733 (1984).

[2] V. F. Nesterenko, *Dynamics of Heterogeneous Materials* (Springer-Verlag, New York, 2001).

[3] C. Coste, E. Falcon, and S. Fauve, Phys. Rev. E **56**, 6104 (1997).

[4] S. Sen, J. Hong, J. Bang, E. Avalos, and R. Doney, Phys. Rep. **462**, 21 (2008).

[5] J. Hong and A. Xu, Appl. Phys. Lett. **81**, 4868 (2002).

[6] C. Daraio, V. F. Nesterenko, E. B. Herbold, and S. Jin, Phys. Rev. E **72**, 016603 (2005).

[7] C. Daraio and V. F. Nesterenko, Phys. Rev. E **73**, 026612 (2006).

[8] V. F. Nesterenko, C. Daraio, E. B. Herbold, and S. Jin, Phys. Rev. Lett. **95**, 158702 (2005).

[9] C. Daraio, V. F. Nesterenko, E. B. Herbold, and S. Jin, Phys. Rev. E **73**, 026610 (2006).

[10] M. A. Porter, C. Daraio, I. Szelengowicz, E. B. Herbold, and P. G. Kevrekidis, Physica D **238**, 666 (2009).

[11] D. Khatri, C. Daraio, and P. Rizzo, Proc. SPIE **7292**, 72920P (2009).

[12] J. Hong, J. Y. Ji, and H. Kim, Phys. Rev. Lett. **82**, 3058 (1999).

[13] J. Hong, Phys. Rev. Lett. **94**, 108001 (2005).

[14] S. Job, F. Melo, A. Sokolow, and S. Sen, Phys. Rev. Lett. **94**, 178002 (2005).

[15] L. Vergara, Phys. Rev. Lett. **95**, 108002 (2005).

[16] G. Theocharis, M. Kavousanakis, P. G. Kevrekidis, C. Daraio, M. A. Porter, and I. G. Kevrekidis, Phys. Rev. E **80**, 066601 (2009).

[17] F. Fraternali, M. A. Porter, and C. Daraio, Mech. Adv. Mater. Struct. **17**, 1 (2010).

[18] R. Carretero-González, D. Khatri, M. A. Porter, P. G. Kevrekidis, and C. Daraio, Phys. Rev. Lett. **102**, 024102 (2009).

[19] X. Ni, P. Rizzo, and C. Daraio, Proc. SPIE **7292**, 729218 (2009).

[20] A. Spadoni and C. Daraio, Proc. Natl. Acad. Sci. USA **107**, 7230 (2010).

[21] J.-D. Aussel and J.-P. Monchalin, Ultrasonics **27**, 165 (1989).

[22] S.-C. Wooh and Q. Zhou, J. Appl. Phys. **89**, 3469 (2001).

[23] F. Lanza di Scalea, P. Rizzo, and A. Marzani, J. Acoust. Soc. Am. **115**, 146 (2004).

[24] C. Thomsen, H. T. Grahn, H. J. Maris, and J. Tauc, Phys. Rev. B **34**, 4129 (1986).

[25] C. B. Scruby and L. E. Drain, in *Laser Ultrasonics: Techniques and Applications* (Adam Hilger, Bristol, 1990), pp. 223–324.

[26] X. Ni, P. Rizzo, and C. Daraio, Rev. Sci. Instrum. **82**, 034902 (2011).